Limnol. Oceanogr., 41(6), 1996, 1253–1263

Phytoplankton photosynthetic characteristics from fluorescence induction assays of individual cells

Robert J. Olson, Alexander M. Chekalyuk, and Heidi M. Sosik
Biology Department, Woods Hole Oceanographic Institution, Woods Hole, Massachusetts 02543-1049

Abstract

Saturating-flash fluorescence techniques, which can provide information about the physiological state of phytoplankton, at present measure bulk water samples and so provide "averaged" values for all the fluorescent particles present. In analyzing natural samples, however, more detailed information about the distribution of photosynthetic characteristics among different cell types and(or) individual cells is desirable. Therefore we developed two methods for applying a "pump-during-probe" technique on a cell-by-cell basis. We used either an epifluorescence microscope or a flow cytometer to make time-resolved measurements of the increase in chlorophyll fluorescence induced by a rectangular excitation pulse of 100-μs duration. We used a biophysical model of fluorescence induction to obtain information about the quantum yield of photochemistry in photosystem 2 (PS2) and the functional absorption cross-section for PS2. For several species (including the smallest phytoplankton, *Prochlorococcus*, which are 0.7 μm in diameter), the maximum quantum yield of photochemistry in PS2 obtained by averaging data from many individual cells agreed well with estimates derived from bulk measurements of DCMU enhancement of Chl fluorescence.

Saturating-flash fluorescence measurements such as "pump-and-probe" (Kolber and Falkowski 1993; Gorbunov et al. 1991), "fast repetition rate" (FRR) (Falkowski and Kolber 1995), and "pulse amplitude modulation" (Hofstraat et al. 1994) are increasingly widely used to monitor the state of the photosynthetic apparatus in phytoplankton under natural conditions. These techniques are based on observing the increase in fluorescence yield of chlorophyll caused by excitation conditions that close reaction centers (RCs) at an appropriate rate. Both pump-and-probe and FRR techniques have recently been applied to oceanographic research questions involving spatial and temporal variability of photosynthetic characteristics in the ocean (Falkowski and Kolber 1995) and the limitation of phytoplankton growth by nitrogen and iron (Kolber et al. 1990, 1994).

At present these are bulk water measurements, so the results represent weighted average properties of all the fluorescent particles present in a sample. Because cells of different types or with different histories may respond to a given environment in different ways, the ability to examine individual cells would provide improved resolution. It would also allow us to avoid potential artifacts caused by fluorescence from nonphotosynthetically-active material (dead cells, detritus, fecal material, grazers with ingested phytoplankton cells). For example, in a bulk measurement, an increasing proportion of detrital chlorophyll and an increasing degree of N limitation would both appear as a decrease in photosynthetic performance; measurements made on a cell-by-cell basis would be unaffected by detrital chlorophyll.

One way to approach measurements of individual cells is with flow cytometry. The potential for flow cytometric measurement of photochemical energy conversion efficiency of photosystem 2 (PS2) in phytoplankton cells was demonstrated with a pump-and-probe approach (Olson and Zettler 1995), although the results suggested that its utility would be limited by sensitivity problems associated with the low excitation intensity required for probing. In this paper we describe an improved approach for single-cell measurements that provides higher sensitivity and additional information about absorption characteristics. This approach is essentially a fluorescence induction measurement (rather than a single probe measurement) on the time scale of 30–100 μs. At this time scale, which is shorter than the turnover time of PS2 RCs but longer than the lifetime of light-induced fluorescence quenchers, it is possible to use a simple analytical model to obtain quantitative information about primary photochemical reactions in PS2. To emphasize the similarities of time scale (less than RC turnover time) and excitation intensity (sufficient to close most if not all RCs) to those of the original pump-and-probe technique introduced by Mauzerall (1972) for studying fluorescence kinetics in vivo, we refer to our approach as "pump-during-probe" (PDP).

The PDP approach was implemented in a microscope system and in a flow cytometer. In each application, we measured the time-course of chlorophyll fluorescence yield during a continuous, rectangular excitation pulse (100-μs duration) of blue light. Fluorescence was detected with a photomultiplier tube (PMT) and recorded with a digital oscilloscope; for very small cells, time-resolved photon counting was used. The results provide information about the maximum quantum yield of photochemistry in PS2

Acknowledgments

We thank Paul Falkowski, Zbigniew Kolber, and Bob Auer for helpful discussions and advice. We thank Maxim Gorbunov for his contributions to the model approach and Emil Bergeron for the LED controller.

This work was supported by EPA grant 010593/530822 and DOE grant DE-FG02-93ER61693 (to R.J.O.), and a DOE Global Change distinguished postdoctoral fellowship (to H.M.S.).

Woods Hole Oceanographic Institution Contribution 9340.

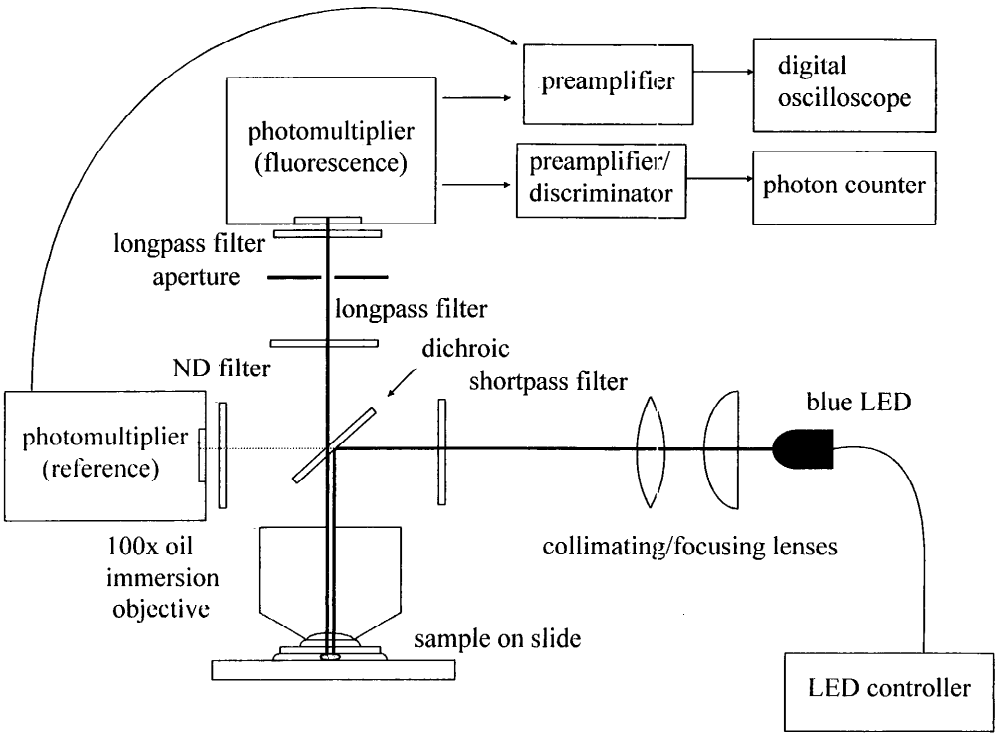

Fig. 1. Schema of the microscope-based pump-during-probe system.

and the functional absorption cross-section for PS2 and will be useful for estimating the contribution of different groups of phytoplankton to photosynthetic activity in the ocean.

Methods

Cultures—Batch cultures of the diatoms *Thalassiosira weissflogii* (clone Actin) and *Phaeodactylum tricornutum* (clone Phaeo), the chlorophytes *Dunaliella tertiolecta* (clone Dun) and *Nannochloris* sp., and the coccolithophores *Emiliania huxleyi* (clone 12-1) and *Syracosphaera elongata* (clone SE-62) were grown in f/2 medium (Guillard 1975) at 20°C under continuous illumination ("cool-white" fluorescent, 100 μmol photons m^{-2} s^{-1}). The procaryotic picoplankter *Prochlorococcus marinus* (strain FP-12) was grown in K/10 medium (Moore et al. 1995) at 24°C under continuous illumination ("warm-white" fluorescent, 15 μmol photons m^{-2} s^{-1}). All cultures were kept in 25×150-mm borosilicate tubes, and growth was monitored by measuring in vivo fluorescence with a Turner Designs model 10 fluorometer.

DCMU treatment—To verify quantitatively the PDP measurements, we compared these results to parallel bulk measurements of fluorescence enhancement by DCMU (3-[3,4-dichlorophenyl]-1,1-dimethyl urea), which prevents the reoxidation of the primary electron acceptor of PS2. An 8-ml sample of culture was dark adapted for 15 min, and its fluorescence measured with a Turner Designs fluorometer (Φ_0). DCMU (4 mM in ethanol) was then added to a final concentration of 5 μM and the sample placed in the light for 1–2 min before remeasuring fluorescence (Φ_m).

Microscope-based measurements—A modified epifluorescence microscope (Zeiss) was used to assay phytoplankton cells on microscope slides (Fig. 1). A cell (observed with a 100× Neofluar objective and bright-field illumination) was positioned in the center of the field of view, after which the cell was dark adapted for 2–5 min. Fluorescence was excited by a single rectangular pulse from a blue LED (emission 470 nm, NLPB500, Nichia America Corp.) positioned in place of the normal Hg arc lamp. The duration and intensity of the blue flash were controlled by a custom circuit based on a 555 timer chip and a field effect transistor. Typically the pulse current through the LED (which is rated at 100 mA for a 10-ms pulse) was 300 mA for 100 μs. To monitor the excitation flash, we placed a PMT screened by a neutral density filter (ND 2) at the window normally used to view the arc lamp for alignment and focusing. Zeiss filter set 487709 allowed blue excitation light to illuminate the sample and red chlorophyll fluorescence to pass up the camera tube to a second PMT (Hamamatsu R1477). An interference filter (680DF40, Omega Optical, Inc.) was placed in front of the fluorescence PMT to further reduce stray excitation light, and a 1.5-mm aperture at the camera tube ocular limited the field of view of the PMT to 15 μm to minimize the amount of background signal.

Signals from both PMTs were amplified with a fast (300 Mhz) 25× preamplifier (SR445, Stanford Research, Inc.),

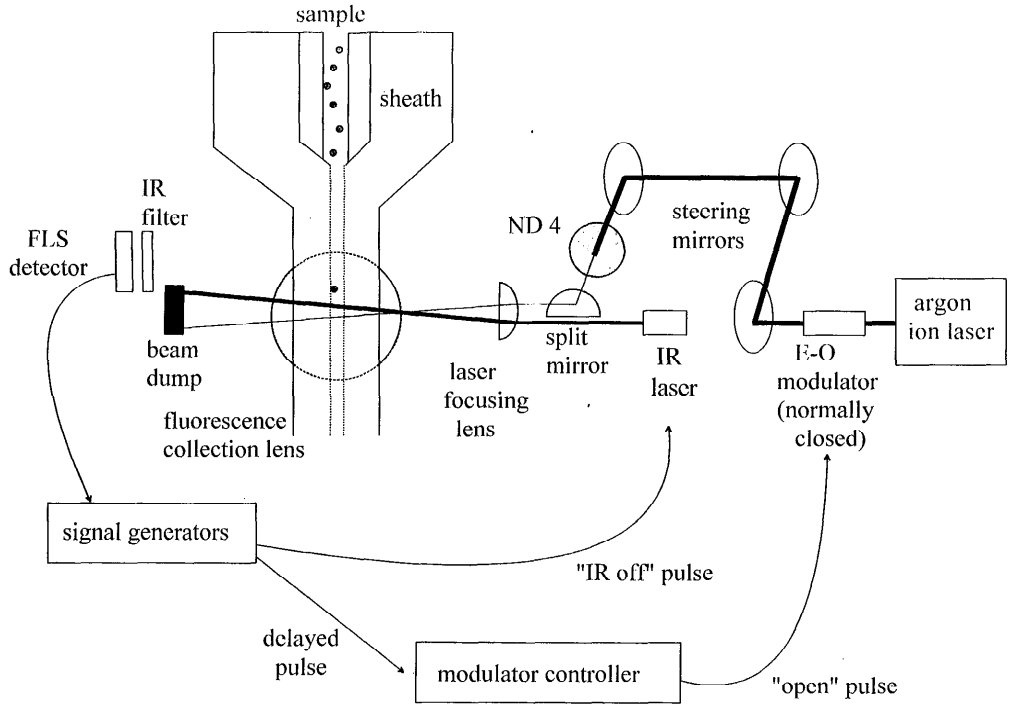

Fig. 2. Schema of the flow cytometer-based pump-during-probe system. PMTs for measuring fluorescence and side-scattered 488-nm laser light (not shown) are located behind the fluorescence collection lens.

smoothed with a resistor-capacitor chain (time constant, 0.25 μs), and recorded at 50-ns intervals with a digital oscilloscope (LeCroy 9314L). The oscilloscope was triggered by the pulse sent to turn on the LED. Data were transferred to a personal computer, where they were further smoothed by averaging across 1-μs intervals. Typical fluorescence signals for *T. weissflogii* (10-μm cells) were ~50–80 mV and 2–4 mV for *Nannochloris* sp. (3-μm cells). Background fluorescence signals, with no cell in the field of view, were <0.5 mV. Nonfluorescent particles (i.e. uncolored 5-μm latex beads or *D. tertiolecta* cells after pigment extraction with methanol) caused no increase in signal above this background level. The dark current from the PMT (obtained by recording the fluorescence signal before the LED pulse) was subtracted from the signals. For each sample, the fluorescence was normalized to the time-course of excitation intensity to give the induction curve of Chl fluorescence yield in relative units. The data were then fitted to a theoretical model to obtain estimates of photosynthetic parameters as described below.

Flow cytometer measurements—A modified Coulter EPICS 753 flow cytometer was used to perform an assay analogous to that described above for the microscope, except that the cells were flowing through the fluorescence assay region (Fig. 2). The excitation pulse was provided by a 488-nm Ar ion laser (Coherent 90-5) whose beam passed through an electro-optic modulator with an opening time of <1 μs (Conoptics, Inc.). Because cells enter the assay region at random times, we used an infrared (IR) cell detector to time the pulse to coincide with the presence of a cell; when a cell passed through the IR beam upstream of the assay region, its forward light scatter signal triggered a circuit that opened the 488-nm beam modulator after the appropriate delay. The IR beam (which was chosen to avoid light-induced change in the dark-adapted state of PS2) was obtained from a diode laser (50 mW, 785 nm; Lasiris Inc.) fitted with an adjustable focusing lens.

To apply a rectangular pulse to a moving cell, we needed a wide and uniform laser beam profile (not the normal Gaussian profile of the Ar ion laser). For the purposes of the exploratory assays described here, we adjusted our existing flow cytometer excitation system to obtain a crude approximation of the desired beam profile; the beam was focused to a width of ~100 μm at the sample using a 38-mm planoconvex lens, and the beam profile was flattened by opening the laser aperture to obtain a mixture of modes. By slowing the sample velocity so that a cell traveled only 20 μm during 100 μs and opening the laser modulator only when a cell was approaching the center of the area to be illuminated by the beam, we were able to obtain nearly constant illumination during the excitation pulse (Fig. 3). With the chosen flow rate and laser spot size, the entire assay region was within the field of view of the fluorescence collection optics, as verified by a narrow (16 μm) beam spot used to illuminate uniform fluorescent microspheres at different positions along the flow cell. Thus, signal size variations during the assay were due to variations in fluorescence emission, not detection efficiency.

Fluorescence time-course data were collected by using

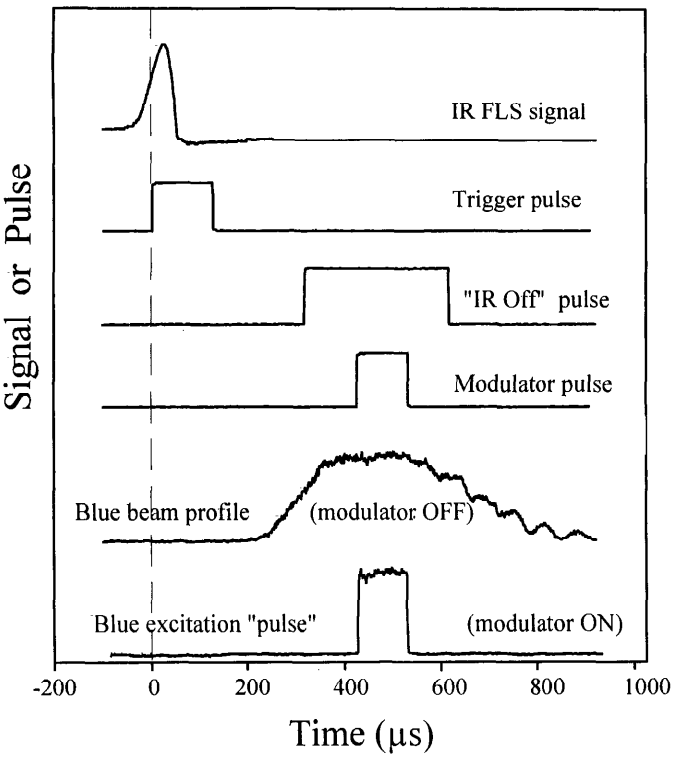

Fig. 3. Sequence of events during flow cytometric fluorescence induction assay. The forward light scattering signal from a cell entering the IR laser beam (IR FLS) exceeds a preset threshold, which causes a trigger pulse. After a preset delay, the IR laser is turned off to avoid interference during the fluorescence assay. The fluorescence signal from a cell traversing the 488-nm laser beam is shown for illustration, with the laser modulator disabled. During the actual assay, the laser modulator is opened after a preset delay to provide an excitation pulse when the cell is near the center of the assay region.

either the same digital oscilloscope as for the microscope-based system (analog mode) or by using a preamplifier/discriminator (F-100E, Advanced Research Instr. Corp.) and a time-resolved photon counting board (MCS-Plus, EG&G Ortec) installed in a personal computer. In analog mode, either individual cell curves or accumulations of sequential measurements could be collected; in photon-counting mode, data from hundreds to thousands of cells were accumulated for each curve. In the latter case, data were obtained with 2-μs resolution.

The shape of the excitation pulse was monitored in two ways. For large cells (>3 μm), we used the time-course of side scattering of laser light by each cell, which should be independent of physiology at these short time scales. Side-scatter signals were obtained with a 488-nm longpass dichroic mirror located after the fluorescence collection lens, and a second PMT. Scattering background was measured (by triggering the laser modulator and signal acquisition system in the absence of cells) and subtracted from the cell data. For small cells, it was not possible to measure side scattering because of the small size of the signals relative to background scattered laser light, so we measured the fluorescence time course of red-fluorescing latex microspheres (1 μm, Molecular Probes), which have no physiology and thus produce signals proportional to the excitation intensity.

The dark current or count rate from the PMT (obtained by recording the fluorescence signal before the laser modulator was opened) was subtracted from the signals; the size of the dark count rate was ~20% that of the fluorescence signal in the worst case (i.e. for the smallest cells, *P. marinus*). The additional background contributed by the laser pulse was very low (<2% of the smallest cells' signals).

The 488-nm laser was typically operated at ~250 mW and attenuated by neutral density filters (OD = 4). Laser power was adjusted to obtain fluorescence rise times of ~30–100 μs. The rate of sample introduction was adjusted to ensure that only one cell was in the blue beam at any given time.

Passage of a cell through the IR beam did not cause any change from the dark-adapted state, as shown by empirical tests in which we monitored fluorescence induction from *D. tertiolecta* and *Nannochloris* cells passing through a continuous 488-nm laser beam and triggering data acquisition directly from fluorescence signals. The fluorescence time-courses were identical whether the IR laser beam was on or off (data not shown).

Data analysis

Interpretation of fluorescence induction measurements requires a model relating the induction curve to photosynthetic parameters of interest, such as the quantum yield and absorption cross section for photochemical energy conversion. There are several theoretical approaches to the description of fluorescence induction (e.g. *see* Sonneveld et al. 1980; Paillotin et al. 1983; Trissl et al. 1993; Trissl and Lavergne 1995), but these do not consider the reopening of RCs and most also require numerical solution of systems of kinetic equations using a number of experimentally determined constants. In previous oceanographic applications, such as pump-and-probe and FRR (which differ somewhat from PDP in experimental protocol), different approaches to data interpretation have been used (*see* Falkowski et al. 1992; Falkowski and Kolber 1995), so we describe ours in some detail.

Fluorescence induction and model assumptions—Almost all Chl fluorescence in vivo originates from PS2 (Krause and Weis 1991), with the yield depending on the concentration of various fluorescence quenchers. When a RC with primary electron acceptor Q_A in the oxidized state (an open RC) captures an exciton, primary charge separation (photochemistry) takes place, followed by reduction of Q_A. The RC is then photochemically inactive (closed) and cannot effectively capture another exciton until Q_A^- is reoxidized (i.e. the RC is re-opened) due to transfer of an electron to the secondary acceptor Q_B (Crofts and Wraight 1983). Because the open RCs are effective quenchers of Chl fluorescence, an increase in the fraction

of closed RCs will cause a rise in fluorescence yield. Closing of RCs is considered the major cause of Chl fluorescence induction upon illumination of dark-adapted samples (Govindjee 1995), although there is a variety of other photochemical and nonphotochemical processes occurring in the photosynthetic apparatus, which result in a polyphasic fluorescence rise over most time scales (Schreiber and Neubauer 1987; Strasser et al. 1995). This complex situation makes it difficult to retrieve quantitative information about PS2 reactions (Govindjee 1995); for example, recent evidence suggests that PS2 photochemical efficiency may be overestimated by measurements at time scales longer than the RC turnover time (Kramer et al. unpubl.; *but see* Schreiber et al. 1995).

Making induction measurements at the time scale of 30–100 μs (i.e. the PDP or FRR approaches) allows us to avoid several of these potentially complicating processes. Because the upper time limit of the measurement is shorter than the turnover time of PS2 RCs (≥150 μs; Kolber et al. 1988), no pronounced changes in the redox state of the RC's acceptor side (Q_B, plastoquinone (PQ) pool) should occur during the induction (aside from the reduction of Q_A). Therefore, decreases in nonphotochemical PQ quenching (sensu Vernotte et al. 1979; Schreiber and Neubauer 1987) should not take place during the measurements. At the donor side of the RCs, the major processes potentially affecting the fluorescence yield are the oxidation of primary electron donor P680 during photochemical charge separation in PS2 RC (Krause and Weis 1991) and the ensuing change in S-state of the oxygen-evolving complex. The lifetime of $P680^+$ is short (<1 μs; Meyer et al. 1989), and in dark-adapted cells the change in S-state that follows the re-reduction of $P680^+$ is relatively slow (half-time > 100 μs; Dekker et al. 1984), so, to a first approximation, both quenching by $P680^+$ (Govindjee 1995; Mauzerall 1972) and S-related changes in the fluorescence yield (Dau 1994; Hsu 1993) can be considered minor at the time scale of 30–100 μs. Finally, the lower limit of the PDP time scale allows us to neglect potential effects of exciton-induced triplet states of carotenoids, whose longest life-time is 7 μs (Breton et al. 1979).

Model description—Chl fluorescence yield Φ_f can be described with the Stern-Volmer equation (Duysens 1979; Paillotin et al. 1983; Shinkarev and Govindjee 1993) in the following form:

$$\Phi_f = k_f/(k_f + k_d + k_p A). \quad (1)$$

A is the fraction of open RCs, and k_f, k_d, and k_p are the rate constants for fluorescence, thermal dissipation, and photochemistry in PS2, respectively. This is reasonable since linear dependence of Φ_f^{-1} on A (as well as other quenchers) has been previously observed (Van Gorkom et al. 1978; Sonneveld et al. 1980; Kingma et al. 1983).

In the dark-adapted state, when all RCs are open (A = 1), the fluorescence yield is minimal:

$$\Phi_0 = k_f/(k_f + k_d + k_p). \quad (2)$$

In contrast, when all RCs are closed ($A = 0$), the maximum fluorescence yield can be expressed as

$$\Phi_m = k_f/(k_f + k_d). \quad (3)$$

From Eq. 1–3, the actual fluorescence yield can be expressed as

$$\Phi_f = [A\Phi_0^{-1} + (1 - A)\Phi_m^{-1}]^{-1}. \quad (4)$$

The rate of change in A is determined by the difference between the rates of RC closing and opening:

$$dA/dt = -\sigma_{PS2} I A + (1 - A)/\tau_A. \quad (5)$$

σ_{PS2} is the functional absorption cross-section of a PS2 RC, I is the intensity of excitation, and τ_A is the apparent time constant for Q_A^- reoxidation due to electron transfer to Q_B.

In deriving a solution to Eq. 5 we have assumed that σ_{PS2} is a constant, which is consistent with experimental results showing that σ_{PS2} does not depend on the fraction of closed RCs (Ley and Mauzerall 1986; Falkowski et al. 1986). Due to the lack of pronounced change in redox states of Q_B and PQ (see above), τ_A may also be considered a constant whose value is determined by the initial proportions of oxidized and reduced Q_B (Crofts et al. 1993). Therefore, for dark-adapted cells (A = 1 at t = 0) which are exposed to continuous and constant excitation, A declines exponentially:

$$A(t) = (\alpha\tau_A)^{-1}[1 + (\alpha\tau_A - 1)\exp(-\alpha\tau)], \quad (6)$$

which is a solution of Eq. 5. The rate constant $\alpha = \sigma_{PS2} I + 1/\tau_A$ is the sum of the rates of exciton trapping by open RCs (closing) and of RC reopening, and the equilibrium between these rates leads to A reaching a steady-state level $A_s = 1/(\alpha\tau_A)$. In the case of strong excitation ($\sigma_{PS2} I \gg 1/\tau_A$), A_s approaches 0 (dynamic closure of all RCs).

Given the assumption that the rate constants k_f, k_d, and k_p do not change over the time scale of our measurements, one can obtain an expression describing Chl fluorescence induction from Eq. 4 and 6:

$$\Phi_f(t) = [\Phi_s^{-1} - (\Phi_s^{-1} - \Phi_0^{-1})\exp(-\alpha\tau)]^{-1} \quad (7)$$

where Φ_s is the fluorescence yield at steady state (i.e. when A reaches A_s):

$$\Phi_s = [\Phi_m^{-1} - (\Phi_m^{-1} - \Phi_0^{-1})/(\alpha\tau_A)]^{-1}. \quad (8)$$

Estimation of photosynthetic parameters—This approach enables us to estimate Φ_p and σ_{PS2} from the measured $\Phi_f(t)$ by means of the following procedure.

1. Determination of Φ_0, Φ_s, and α from $\Phi_f(t)$ using least-squares nonlinear regression to Eq. 7.
2. Calculation of Φ_m from Eq. 8:

$$\Phi_m = (\alpha\tau_A - 1)/(\alpha\tau_A\Phi_s^{-1} - \Phi_0^{-1}). \quad (9)$$

3. Calculation of the maximum potential quantum yield of photochemistry in PS2 (i.e. Φ_p, Krause and Weis 1991) and the functional absorption cross-section of a PS2 RC (i.e. σ_{PS2}):

$$\Phi_p = k_p/(k_f + k_d + k_p) = (\Phi_m - \Phi_0)/\Phi_m; \quad (10)$$

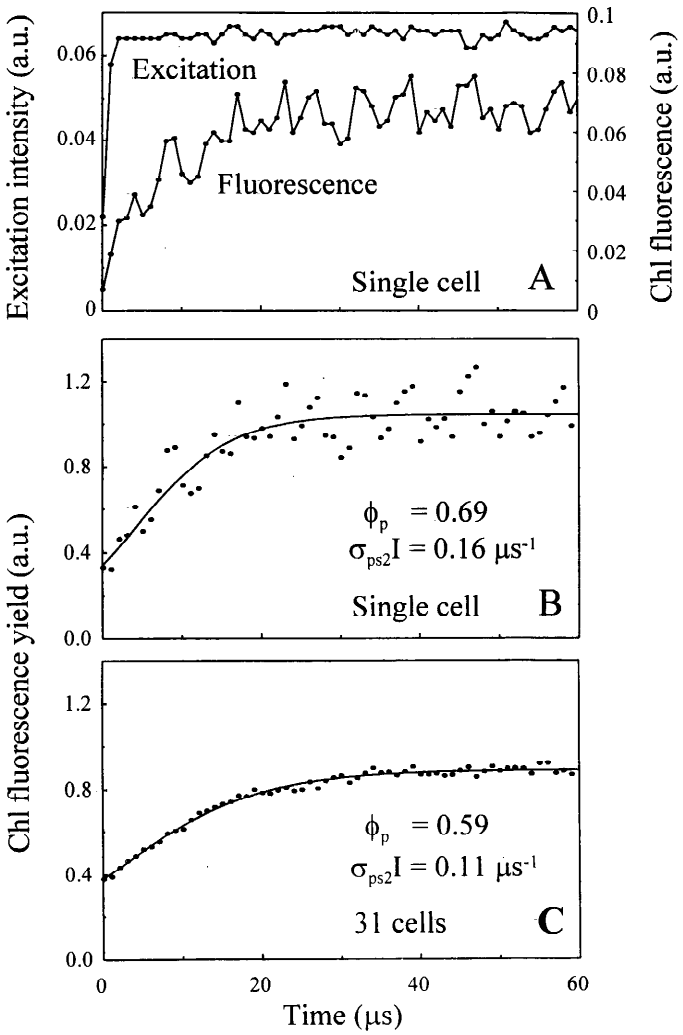

Fig. 4. Fluorescence induction measurements of *Thalassiosira weissflogii* using the microscope-based system. A. Time-course of the intensity of the LED pulse (upper curve) and the resulting chlorophyll fluorescence (lower curve) for a single cell. B. Time-course of fluorescence yield (fluorescence/excitation) for the same cell. C. Fluorescence yield for accumulated data from 31 cells (Φ_p = 0.59). The solid curves in panels B and C and the values of Φ_p and $\sigma_{PS2}I$ are based on model results (Eq. 7–11). The bulk DCMU-based estimate of Φ_p for this sample was 0.63.

$$\sigma_{PS2} = (\alpha - 1/\tau_A)/I. \quad (11)$$

We followed this procedure except that since we did not quantify I, we obtained the product $\sigma_{PS2}I$ rather than absolute values for σ_{PS2}. The product $\sigma_{PS2}I$ [the rate constant for exciton trapping by RCs (quanta s^{-1} per RC)] is useful for comparing absorption cross-sections in relative units.

A value of τ_A is required for this procedure. Based on published results (e.g. Robinson and Crofts 1983; Crofts et al. 1993; Wollman 1978), we estimated τ_A as 240 μs. This value was derived by computer simulation assuming two oxidation states of Q_B with time constants for Q_A^- reoxidation of 145 and 600 μs present in equal proportions in the dark-adapted state. Although variations in the relative abundance of these Q_B oxidation states in different species or in cells of different physiological status (Kolber et al. 1988) may change the τ_A value, this will not greatly affect the accuracy of estimates of photosynthetic parameters due to the relatively minor contribution of Q_A^- reoxidation at the PDP time scale. For example, a 2.5-fold change in the relative contributions of the components with 145- and 600-μs time constants (as for N-starved vs. nutrient-replete *D. tertiolecta* cells reported by Kolber et al. 1988, their figure 4) would result in <5% difference in the estimates of Φ_p and σ_{PS2} obtained with our model.

The model suggests that the reopening of RCs during the measurements can affect the estimates of photosynthetic parameters. Because the potential photochemical yield Φ_p of PS2 is determined by the ratio $(\Phi_m - \Phi_0):\Phi_m$, an underestimation of Φ_p would result from the use of Φ_s rather than Φ_m (i.e. $\Phi_{p,s} = [\Phi_s - \Phi_0]/\Phi_s$). From Eq. 8, the relative difference is $(\Phi_p - \Phi_{p,s})/\Phi_p = (\alpha\tau_A)^{-1}$. Assuming τ_A = 240 μs, as we did, $(\Phi_p - \Phi_{p,s})/\Phi_p$ will be 2% when the rise time is 30 μs (α = 0.20) and 7% when the rise time is 100 μs (α = 0.06). It is also possible to assume that $1/\tau_A$ is negligible when calculating the functional absorption cross-section in Eq. 11. This would result in overestimation of σ_{PS2}, again in the range of 2–7% at the induction time scale of 30–100 μs.

Results and discussion

Microscope-based PDP measurements—The fluorescence signals from relatively large cells such as *T. weissflogii* (a 10-μm diatom) were large enough that we could estimate photosynthetic characteristics from a single measurement, although the signal-to-noise ratio could be increased by using data from more than one cell (Fig. 4). Similar results were obtained with *D. tertiolecta*, a 7-μm cell (data not shown). With smaller species, signal to noise decreased. For example, with *Nannochloris* (a 3-μm cell), the fluorescence data from individuals were so noisy that we considered population averaging necessary to obtain reliable estimates of photosynthetic parameters.

Diversity in photosynthetic characteristics among cells—The microscope-based PDP system can be used to analyze both cell-to-cell and species diversity in photosynthetic characteristics. When we examined a *T. weissflogii* culture that was just entering N-limited stationary phase (after transfer to N-free medium), for example, we observed much higher cell-to-cell diversity than in a nutrient-replete exponential culture. Three cells chosen from a single slide exhibited values for the quantum yield of photochemistry in PS2 (Φ_p) that spanned nearly the entire range from photochemically inactive to fully functional (Fig. 5). At the same time, the value of Φ_p calculated from accumulated signals from 31 cells (0.45) was close to the bulk value calculated from measurements of DCMU enhancement of fluorescence (0.51), indicating that the sam-

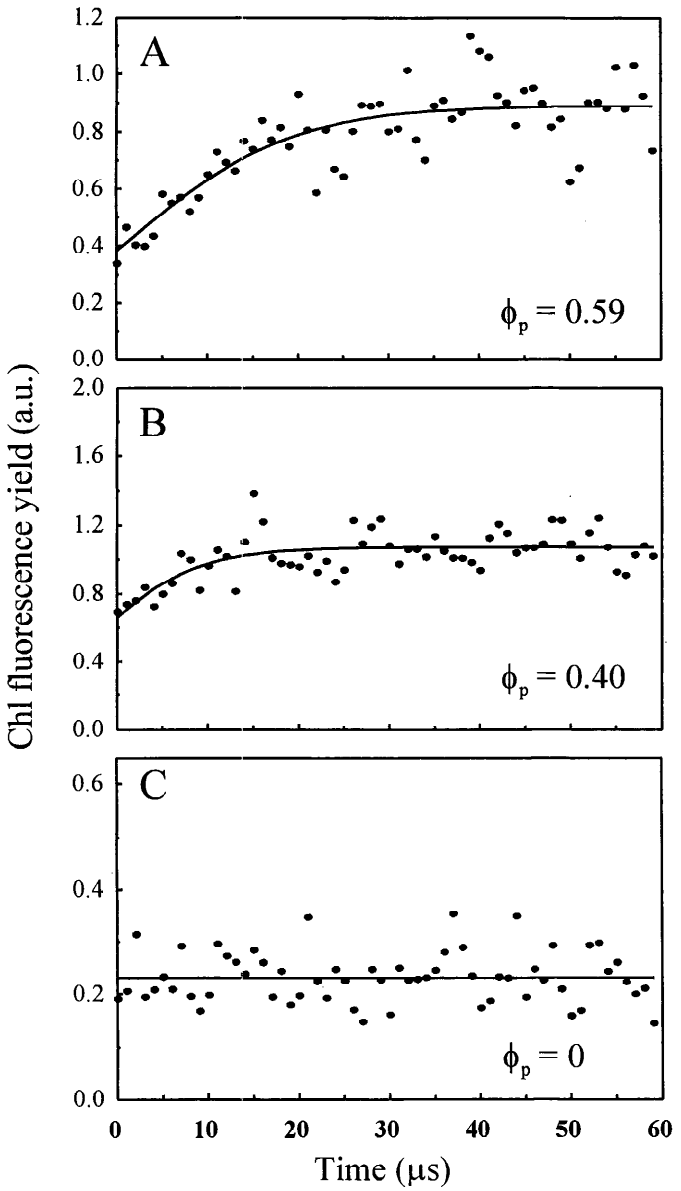

Fig. 5. Increase in chlorophyll fluorescence yield measured with the microscope-based system for three *Thalassiosira weissflogii* cells (A, B, C) from a culture transferred 3 d earlier to N-free medium. The solid curves and the values of Φ_p are based on model results.

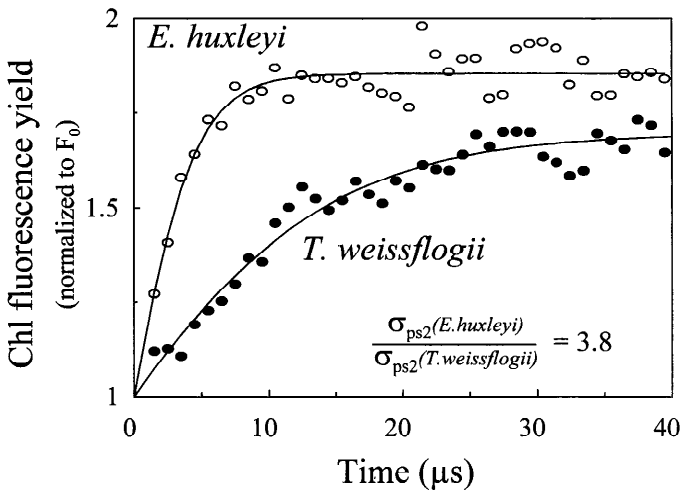

Fig. 6. Fluorescence induction measurements of *Emiliania huxleyi* and *Thalassiosira weissflogii* (31 cells each) obtained with the microscope-based PDP system. The solid curves are model results. The measurements were all made with the same excitation intensity, so the observed difference in $\sigma_{PS2}I$ between the two cultures (0.42 vs. 0.11 μs^{-1}) reflects a difference in absorption cross-section for PS2.

ple was representative of the bulk culture. The value of $\sigma_{PS2}I$ (the exciton trapping rate) was ~0.1 quanta μs^{-1} per RC for the cells in this sample.

In the course of our measurements we also observed variability in absorption cross-sections for PS2 (σ_{PS2}). For example, based on several measurements it was apparent that *E. huxleyi* had higher values for σ_{PS2} than did other species grown under similar conditions (Fig. 6). This difference could reflect either more antennae pigment per PS2 RC or a higher proportion of pigments absorbing 488-nm light in *E. huxleyi* than in other species. We observed a range of more than 4-fold in σ_{PS2} across the six species we tested. This points out the importance of making individual cell measurements in the field. It also implies that when excitation intensity is fixed, the difference between Φ_m and Φ_s will vary from cell to cell in a natural sample, which must be taken into account for best accuracy (*see Eq. 9–11*).

These examples suggest that the PDP technique will allow investigations of population diversity both at the species level and at the individual cell level (at least for cells >5 μm). These capabilities will be especially useful in studies of such phenomena as microenvironments and the redistribution of cells through water-column mixing, for which bulk samples might be difficult to interpret.

Flow cytometer-based PDP measurements—Although the microscope-based system has the valuable feature of allowing the operator to visually examine each cell before analysis, the need to locate and dark-adapt each cell makes the analysis of populations of cells very slow. Flow cytometry, conversely, can resolve phytoplankton only to relatively coarse groups based on light scattering and pigment fluorescence characteristics (Olson et al. 1989; Furuya and Li 1992), but is very rapid. For example, several minutes were sufficient to analyze 1,000 *D. tertiolecta* cells (Fig. 7) and arrive at a value for Φ_p of 0.64, which is virtually identical to that obtained by a bulk DCMU assay ($\Phi_p = 0.66$).

We note that it is also possible to analyze the individual cell data from the flow cytometer from these relatively large cells in the same way as for the microscope (although we did not do so here). Even without the ability to resolve species, such measurements of the distribution of photosynthetic characteristics within a population could be of interest when populations are well defined, such as during algal blooms.

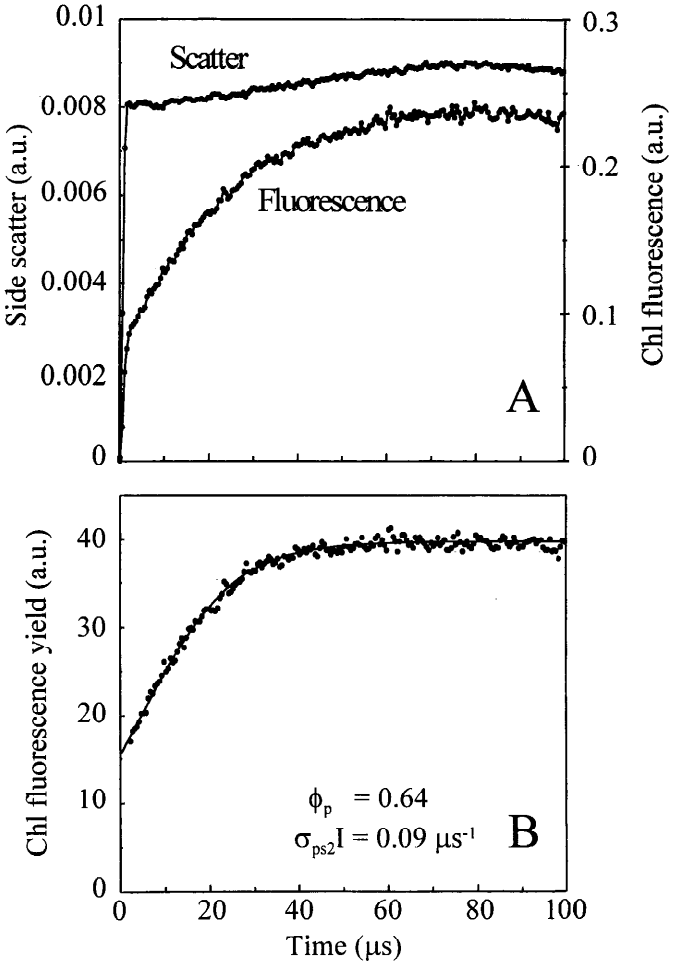

Fig. 7. Fluorescence induction measurements of *Dunaliella tertiolecta* (1,000 cells accumulated) using the flow cytometer-based system with analog acquisition. A. Time-course of the intensity of chlorophyll fluorescence and of side-scattered blue laser light (after subtraction of background). B. Time-course of relative fluorescence yield (fluorescence normalized to scatter). The solid curve in panel B and the values of Φ_p and $\sigma_{PS2}I$ are based on model results.

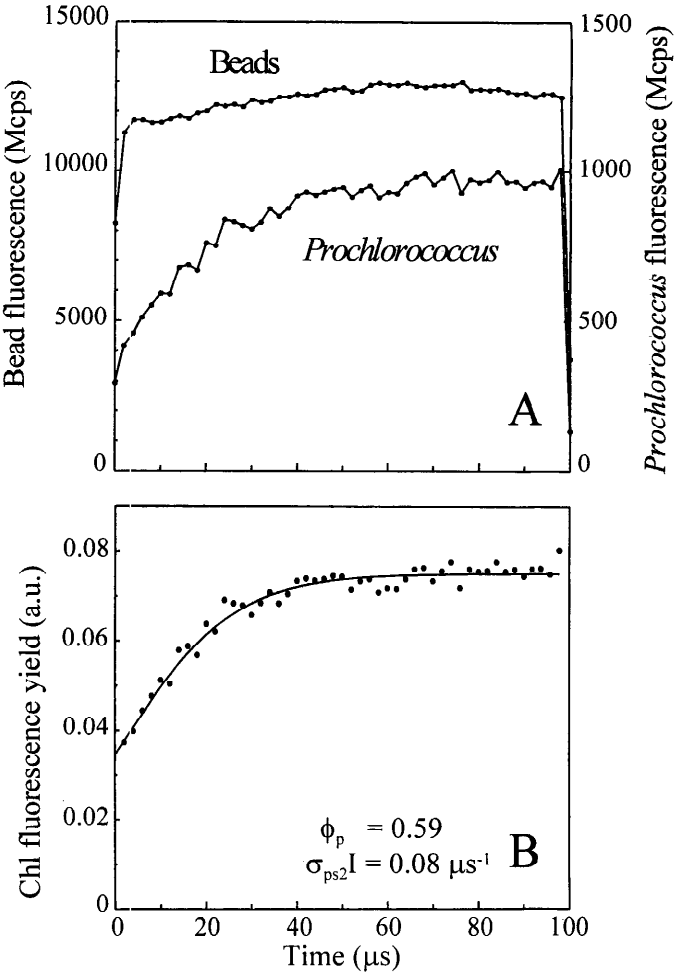

Fig. 8. Fluorescence induction measurements of *Prochlorococcus marinus* (20,000 cells accumulated) using the flow cytometer based system with time-resolved photon counting. A. Time-course of the intensity of chlorophyll fluorescence from the cells and of red fluorescence from 1-μm-diameter fluorescent microspheres used as a reference. B. Time-course of relative fluorescence yield (cell fluorescence normalized to bead fluorescence). The curve in panel B and the values of Φ_p and $\sigma_{PS2}I$ are based on model results.

Estimates of absorption cross section—Although we did not directly measure the intensity of excitation in the PDP flow cytometer, we do know the laser power and the approximate size of the beam at the flow cell. From these data we can estimate that the intensity of excitation is in the range 10^{22}–10^{23} quanta m^{-2} s^{-1}, which leads to σ_{PS2} values in the range of 10^{-18}–10^{-17} m^2 (Eq. 11) for the species we examined. This range is consistent with data obtained for marine phytoplankton with independent bulk techniques (e.g. Mauzerall and Greenbaum 1989; Kolber and Falkowski 1993; Dubinsky et al. 1986). Better assessment of the excitation fluence rate (e.g. based on fluorescence saturation of organic dyes) would allow us to obtain more precise estimates of σ_{PS2} and to compare these estimates with independent measurements such as FRR.

Photon counting—For very small cells ($\lesssim$3 μm), fluorescence signals were too small to obtain adequate results by analog data acquisition, even with population averaging. Time-resolved photon counting, however, allowed us to extend the range of measurements to even the smallest phytoplankton cells, *Prochlorococcus,* which are 0.7 μm in diameter. On average, we detected only 2.5 photons from each *Prochlorococcus* cell during its assay, but this signal was about five times higher than the background, so we could obtain a useful induction curve by accumulating data from many cells (Fig. 8). The results could be further improved by using a cooled PMT to reduce the background count rate.

The upper cell size limit for photon counting in our system (determined by the time resolution of the counting

system and the rate of photon emission) is roughly at the size range of *Nannochloris* (3-μm diam), for which parallel analog and photon-counting measurements resulted in virtually indistinguishable fluorescence induction curves (data not shown).

Photon counting can be carried out with either the microscope or the flow cytometer system, but the need to accumulate data from thousands of cells makes the flow cytometer the approach of choice for small cells. An alternative we explored for increasing sensitivity for small cells on the microscope system is to accumulate the results of repeated measurements on the same cell. This method proved infeasible, however, because failure to dark adapt for at least 10 s between repeated measurements on the same cell resulted in complex patterns of fluorescence induction that are difficult to interpret (data not shown). Similar results for data obtained with repeated pulses have been observed by others (e.g. *see* figure 4 of Duysens 1979). This problem is avoided with the flow cytometer, which continually samples new (dark adapted) cells.

Comparison of individual cell and bulk assays—For six species of phytoplankton grown under different conditions, estimates of the quantum yield of photochemistry in PS2 by PDP measurements made on individual cells were well correlated with estimates derived from DCMU-enhancement measurements of bulk samples (Fig. 9). The regression was not forced through zero, but we did observe samples with zero quantum efficiency as measured by both PDP and DCMU approaches, so our data span the entire range of Φ_p values previously observed for phytoplankton (Kolber and Falkowski 1993). There were no obvious differences between the two PDP instruments or among the six species tested. These results indicate that our model assumptions are reasonable and that the microscope- and flow cytometer-based PDP techniques, when applied to individual cells, provide reliable information about the photosynthetic characteristics of phytoplankton.

Future directions—This work has shown that it is possible to obtain population estimates of photosynthetic parameters for even the the smallest phytoplankton from measurements of individual cells, and for larger species to measure photosynthetic characteristics of individuals. To make the technique practical for field studies with natural populations, however, there are two improvements to consider. The first concerns the necessity to identify each cell as it is assayed (both for studies of particular species of large cells and to allow population averaging of smaller cells), and the second, the speed of analysis. The microscope offers the possibility of species identification (at least for larger cells), but it is slow due to the need to manually locate, focus on, and dark-adapt each cell. Implementation of automated cell searching, detection, and identification protocols that use IR illumination and image-processing techniques could allow measurements on many more cells than at present. Flow cytometry is much more rapid than microscopy (thus allowing the analysis of small cells by accumulating data from many individuals), but it cannot identify individuals to the species level. However, several phytoplankton cell types can be recognized from their flow cytometric "signatures," including the smallest cells, which cannot be recognized by microscopy. We therefore plan to add to the flow system described here the capability to measure conventional flow cytometric light scattering and fluorescence parameters downstream of the measurement of photosynthetic parameters.

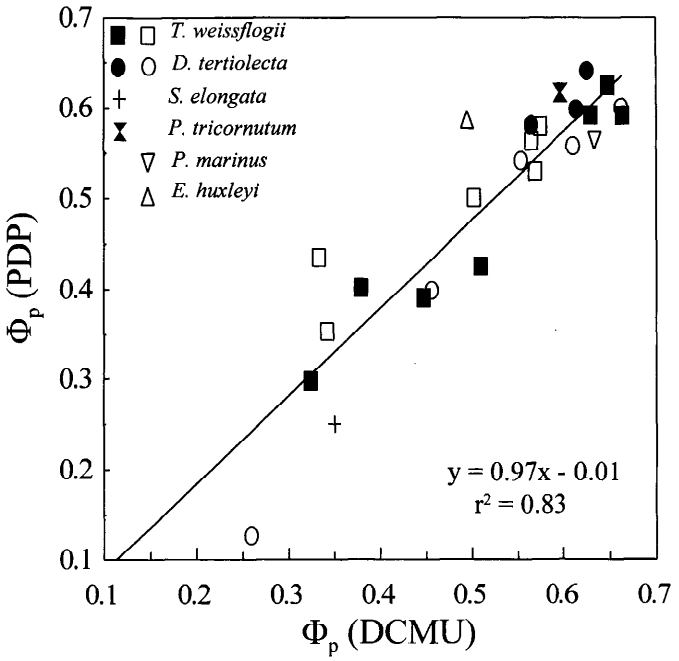

Fig. 9. Correlation between estimates of the quantum yield of photochemistry in PS2 from bulk measurements of DCMU fluorescence enhancement and from individual cell fluorescence induction measurements (PDP) of six species of phytoplankton. The individual cell data are population averages (30–20,000 cells) from both microscope-based (solid symbols) and flow cytometer-based (open symbols) instruments. *Prochlorococcus marinus* was analyzed by photon counting in the flow cytometer. The equation and solid line represent the linear regression, which is close to 1 : 1.

The combined use of the two instruments described here should be a powerful tool for investigating the regulation of phytoplankton growth and for estimating contributions of different groups of phytoplankton to primary production in the sea.

References

BRETON, J., N. E. GEACINTOV, AND C. E. SWENBERG. 1979. Quenching of fluorescence by triplet excited states in chloroplasts. Biochim. Biophys. Acta **548:** 616–635.

CROFTS, A. R., I. BAROLI, D. M. KRAMER, AND S. TAOKA. 1993. Kinetics of electron transfer between Q_A and Q_B in wild type and herbicide-resistant mutants of *Chlamydomonas reinhardtii*. Z. Naturforsch. **48c:** 259–266.

———, AND C. A. WRAIGHT. 1983. The electrochemical do-

main of photosynthesis. Biochim. Biophys. Acta **726:** 149–185.

DAU, H. 1994. Molecular mechanisms and quantitative models of variable photosystem II fluorescence. Photochem. Photobiol. **60:** 1–23.

DEKKER, J. P., J. J. PLIJTER, L. OUWEHAND, AND H. J. VAN GORKOM. 1984. Kinetics of manganese redox transition in the oxygen-evolving apparatus of photosynthesis. Biochim. Biophys. Acta **767:** 176–179.

DUBINSKY, Z., P. G. FALKOWSKI, AND K. WYMAN. 1986. Light harvesting and utilization by phytoplankton. Plant Cell Physiol. **27:** 1335–1349.

DUYSENS, L. N. M. 1979. Transfer and trapping of excitation energy in photosystem II, p. 323–340. *In* Chlorophyll organization and energy transfer in photosynthesis. Ciba Found. Symp. 61 (N.S.). Elsevier.

FALKOWSKI, P. G., R. M. GREENE, AND R. J. GEIDER. 1992. Physiological limitations on phytoplankton productivity in the ocean. Oceanography **5:** 84–91.

———, AND Z. KOLBER. 1995. Variations in chlorophyll fluorescence yields in phytoplankton in the world oceans. Aust. J. Plant Physiol. **22:** 341–355.

———, K. WYMAN, A. LEY, AND D. MAUZERALL. 1986. Relationship of steady-state photosynthesis to fluorescence in eucaryotic algae. Biochim. Biophys. Acta **849:** 183–192.

FURUYA, K., AND W. K. W. LI. 1992. Evaluation of photosynthetic capacity in phytoplankton by flow cytometric analysis of DCMU-enhanced chlorophyll fluorescence. Mar. Ecol. Prog. Ser. **88:** 279–287.

GORBUNOV, M. Y., V. V. FADEEV, AND A. M. CHEKALYUK. 1991. Method for remote laser monitoring of photosynthetic efficiency in phytoplankton. Moscow Univ. Phys. Bull. **46:** 59–65.

GUILLARD, R. R. L. 1975. Culture of phytoplankton for feeding marine invertebrates, p. 29–60. *In* W. L. Smith and M. H. Chaney [eds.], Culture of marine invertebrate animals. Plenum.

GOVINDJEE. 1995. Sixty-three years since Kautsky: Chlorophyll *a* fluorescence. Aust. J. Plant Physiol. **22:** 131–160.

HOFSTRAAT, J. W., J. C. H. PEETERS, J. F. H. SNEL, AND C. GEEL. 1994. Simple determination of photosynthetic efficiency and photoinhibition of *Dunaliella tertiolecta* by saturating pulse fluorescence measurements. Mar. Ecol. Prog. Ser. **103:** 187–196.

HSU, B. D. 1993. Evidence for the contribution of the S-state transition of oxygen evolution to the initial phase of fluorescence induction. Photosynth. Res. **36:** 81–88.

KINGMA, H., L. N. M. DUYSENS, AND R. VAN GRONDELLE. 1983. Magnetic field-stimulated luminescence and a matrix model for energy transfer. Biochim. Biophys. Acta **725:** 434–443.

KOLBER, Z. S., AND OTHERS. 1994. Iron limitation of phytoplankton photosynthesis in the equatorial Pacific Ocean. Nature **371:** 145–149.

———, AND P. G. FALKOWSKI. 1993. Use of active fluorescence to estimate phytoplankton photosynthesis in situ. Limnol. Oceanogr. **38:** 1646–1665.

———, K. WYMAN, AND P. G. FALKOWSKI. 1990. Natural variability in photosynthetic energy conversion efficiency: A field study in the Gulf of Maine. Limnol. Oceanogr. **35:** 72–79.

———, J. ZEHR, AND P. G. FALKOWSKI. 1988. Effects of growth irradiance and nitrogen limitation on photosynthetic energy conversion in photosystem II. Plant Physiol. **88:** 923–929.

KRAUSE, G. H., AND E. WEIS. 1991. Chlorophyll fluorescence and photosynthesis: The basics. Annu. Rev. Plant Physiol. Plant Mol. Biol. **42:** 313–349.

LEY, A., AND D. MAUZERALL. 1986. The extent of energy transfer among photosystem II reaction centers in *Chlorella.* Biochim. Biophys. Acta **850:** 234–248.

MAUZERALL, D. 1972. Light-induced fluorescence changes in *Chlorella,* and the primary photoreactions for the production of oxygen. Proc. Natl. Acad. Sci. **69:** 1358–1362.

———, AND N. L. GREENBAUM. 1989. The absolute size of a photosynthetic unit. Biochim. Biophys. Acta **974:** 119–140.

MEYER, B., E. SCHLODDER, J. P. DEKKER, AND H. T. WITT. 1989. O_2 evolution and Chl a_{II} + (P-680$^+$) nanosecond reduction kinetics in single flashes as a function of pH. Biochim. Biophys. Acta **974:** 36–43.

MOORE, L. R., R. GOERICKE, AND S. W. CHISHOLM. 1995. Comparative physiology of *Synechococcus* and *Prochlorococcus*: Influence of light and temperature on growth, pigments, fluorescence and absorptive properties. Mar. Ecol. Prog. Ser. **116:** 259–275.

OLSON, R. J., AND E. R. ZETTLER. 1995. Potential of flow cytometry for "pump and probe" fluorescence measurements of phytoplankton photosynthetic characteristics. Limnol. Oceanogr. **40:** 816–820.

———, ———, AND O. K. ANDERSON. 1989. Discrimination of eukaryotic phytoplankton cell types from light scatter and autofluorescence properties measured by flow cytometry. Cytometry **10:** 636–643.

PAILLOTIN, G., N. E. GEACINTOV, AND J. BRETON. 1983. A master equation theory of fluorescence induction, photochemical yield, and singlet-triplet exciton quenching in photosynthetic systems. Biophys. J. **44:** 65–77.

ROBINSON, H. R., AND A. R. CROFTS. 1983. Kinetics of the oxidation-reduction reactions of the photosystem II quinone acceptor complex, and the pathway for deactivation. FEBS (Fed. Eur. Biol. Soc. Lett. **153:** 221–226.

SHINKAREV, V. P., AND GOVINDJEE. 1993. Insight into the relationship of chlorophyll *a* fluorescence yield to the concentration of its natural quenchers in oxygenic photosynthesis. Proc. Natl. Acad. Sci. **90:** 7466–7469.

SCHREIBER, U., H. HORMANN, C. NEUBAUER, AND C. KLUGHAMMER. 1995. Assessment of photosystem II photochemical quantum yield by chlorophyll fluorescence quenching analysis. Aust. J. Plant Physiol. **22:** 209–220.

———, AND C. NEUBAUER. 1987. The polyphasic rise of chlorophyll fluorescence upon onset of strong continuous illumination: 2. Partial control by the photosystem II donor side and possible ways of interpretation. Z. Naturforsch. **42c:** 1255–1264.

SONNEVELD, A., H. RADEMAKER, AND L. N. M. DUYSENS. 1980. Transfer and trapping of excitation energy in photosystem II as studied by chlorophyll a_2 fluorescence quenching by dinitrobenzene and carotenoid triplet. The matrix model. Biochim. Biophys. Acta **593:** 272–289.

STRASSER, R., A. STRIVASTAVA, AND GOVINDJEE. 1995. Polyphasic chlorophyll *a* fluorescence transient in plants and cyanobacteria. Photochem. Photobiol. **61:** 32–42.

TRISSL, H.-W., Y. GAO, AND K. WULF. 1993. Theoretical fluorescence induction curves derived from coupled differential equations describing the primary photochemistry of photosystem II by an exciton-radical pair equilibrium. Biophys. J. **64:** 974–988.

———, AND J. LAVERGNE. 1995. Fluorescence induction from photosystem II: Analytical equations for the yields of pho-

tochemistry and fluorescence derived from analysis of a model including exciton-radical pair equilibrium and restricted energy transfer between photosynthetic units. Aust. J. Plant Physiol. **22:** 183–193.

VAN GORKOM, H. J., M. P. J. PULLES, AND A. L. ETIENNE. 1978. Fluorescence and absorption changes in Tris-washed chloroplasts, p. 135–145. *In* H. Metzner [ed.], Photosynthetic oxygen evolution. Academic.

VERNOTTE C., A. L. ETIENNE, AND J.-M. BRIANTAIS. 1979. Quenching of the system II chlorophyll fluorescence by the plastoquinone pool. Biochim. Biophys. Acta **545:** 519–527.

WOLLMAN, F.-A. 1978. Determination and modification of the redox state of the secondary acceptor of photosystem II in the dark. Biochim. Biophys. Acta **503:** 263–273.

Submitted: 28 June 1995
Accepted: 30 January 1996
Amended: 13 February 1996